

Introduction of multiple γ -ray detection to charged particle activation analysis

J. Goto¹  · M. Oshima² · M. Sugawara³ · Y. Yamaguchi² · C. Bi² · S. Bamba² · T. Morimoto²

Received: 5 July 2017 / Published online: 25 October 2017
© Akadémiai Kiadó, Budapest, Hungary 2017

Abstract Charged particle activation analysis (CPAA) is a rapid method with high accuracy which can analyze multi-elements simultaneously. Since multiple γ -ray detection method is expected to improve the detection efficiency and the signal-to-noise ratio, we study what design of the γ -ray detector array is the most suitable for CPAA. We take up four design candidates and investigated the responses by the radiation simulation code Geant 4. From the results, we have deduced the best design with 5 germanium detectors in close geometry. By inspecting the sensitivity in CPAA, the method is proved to be useful and applicable to 116 nuclides.

Keywords Charged particle activation analysis · Multiple γ -ray detection · Signal-to-noise ratio · Detection limit

Introduction

In general, elemental quantification methods based on activation analysis have the characteristics of a rapid, non-destructive analysis with high accuracy which can handle multi-elements simultaneously. Charged particle activation analysis (CPAA) is a typical example of them [1–12] as well as neutron activation analysis (NAA) which is widely

used. In the previous investigation [13], we have demonstrated that CPAA analysis is possible over the whole elements including the heavy nuclear region, while the determination sensitivity tends to decrease gradually as the target nucleus becomes heavy.

A typical beam needed for CPAA is an 8–15 MeV proton beam with an intensity of 0.1–1 μ A. This kind of the beam can be provided by small accelerators which are commercially available for some medical applications such as positron emission tomography (PET) for cancer therapy. The beams provided by these accelerators are intense enough for CPAA. Nowadays, around 150 PET accelerators are running in Japan [14]. The introduction cost becomes reasonable so that a commercial CPAA facility is possible.

In CPAA and NAA we normally use a single germanium (Ge) detector. In the field of nuclear spectroscopy, an array of Ge detectors is often used to improve γ -ray detection efficiency and sensitivity [15–17]. Furthermore, in the previous investigations [18–30], we found that the γ - γ coincidence method or multiple γ -ray detection method utilizing the array of Ge detectors is effective in improving not only energy resolution in nuclide determination but also the detection limit in the γ -ray spectrum in NAA (for details see [29]). The method is called neutron activation analysis combined with multiple γ -ray detection (NAAMG) [29].

The multiple γ -ray detection method has also been applied to neutron prompt γ -ray analysis (PGA), which is called the multiple prompt γ -ray activation analysis (MPGA) [31–36]. The compound nucleus produced after the neutron capture reaction generally locates at high excitation energy (at several MeV). Prompt γ -rays emitted from such highly excited states generally have high energy and the number of the γ -rays is large reflecting a high level

✉ J. Goto
goto@med.niigata-u.ac.jp

¹ Institute for Research Promotion, Niigata University, Niigata 951-8510, Japan

² Japan Chemical Analysis Center, Sanno 295-3, Inage, Chiba 263-0002, Japan

³ Chiba Institute of Technology, Narashino, Chiba 275-0023, Japan

density in this region. Accordingly, the individual strength would be small. This situation sometimes makes the multiple γ -ray detection method less effective in PGA than in NAA. The merit of PGA is that it covers almost all the stable nuclides, while the applicability of NAA is restricted by the decay properties of produced nuclides, that are half life, γ -ray energy, γ -ray branching ratio and so on. Since CPAA deals with decay γ -rays similarly to those in NAA, we can expect a greater improvement of the detection limit by adopting multiple γ -ray detection method than the case of PGA. Here we study the applicability of the multiple γ -ray detection method to CPAA.

In this paper, we firstly study what design of the γ -ray detector array is the most suitable for CPAA. So far we have developed the GEMINI [37] and GEMINI-II [29] arrays for NAAMG and heavy ion induced in-beam γ -ray spectroscopy experiments, the STELLA array for MPGA and neutron induced in-beam γ -ray spectroscopy experiments in JRR-3 M facility, and the ANNRI array for MPGA and pulsed neutron induced in-beam γ -ray spectroscopy experiments in J-PARC facility. Their detector configurations are optimized for the different purposes and as a result, they are different from one another. Here we will investigate the optimum design for CPAA.

The detection limit is important as the performance of the multiple γ -ray detector array. The detection limit is derived from γ -ray detection efficiency and peak-to-background (signal-to-noise) ratio. We take up candidates of the detector configuration and investigate their performances by deriving the signal-to-noise ratio and detection efficiency, which are evaluated by Monte Carlo simulation code Geant 4.10.2 [38–41]. Based on the results, the optimum design of the multiple γ -ray detector array for CPAA is proposed.

Simulation

Details of CPAA

CPAA utilizing a 8–15 MeV proton beam will soon become possible by small accelerators such as the one for boron neutron capture therapy (BNCT) in the Ibaraki Neutron Medical Research Center (INMRC). In the previous investigation [13], we have shown that the possible reactions in CPAA are mostly (p, n) reactions but the other reactions of (p, α), (p, γ), (p, d), (p, 2n) and (p, t) are also available. The radionuclides generated by these reactions decay mostly by β^- , β^+ or electron capture process. The γ -rays, annihilation γ -rays and X-rays emitted after those decays could be utilized for CPAA. We can apply multiple γ -ray detection method to improve the energy resolution

and the detection limit, since some of these radiations are emitted simultaneously in cascade.

Detector configurations

By taking into account the cost of the introduction and the maintenance suitable for a commercial device, we take up four possible configurations labeled A, B, C and D in Fig. 1 for the multiple γ -ray detector array. The design A is composed of six coaxial Ge detectors, each with a BGO anti-Compton shield. The BGO shield is used to decrease the background due to the Compton scattering in the Ge crystal. A lead collimator is placed before the front face of the BGO shield to prevent the γ -rays from directly entering it from a sample. The design B, C and D consist respectively of 6, 7 and 5 Ge detectors without BGO shields which are arranged so as to surround the sample. It is expected intuitively that the design A might have the highest signal-to-noise ratio and the design C and D might have higher detection efficiency than the others. We performed a realistic simulation to evaluate quantitatively the performance of each configuration and to know which configuration has the best detection limit.

Simulation for the spectrometer configurations

Simulations were performed using Geant 4.10.2 [38–41]. The Ge detector in the simulation were reproduced from the catalogue sheet for a commercially available Ge detector (AMETEK GMX40P4-70-A-S) with detection efficiency of 40% relative to a $\phi 3'' \times 3''$ NaI scintillation detector. The BGO scintillation detector used in the simulation was manufactured by Saint-Gobain SA. The Ge detector and BGO shield for the simulation were reproduced from the drawing provided by the manufacture as detailed as possible as shown in Fig. 2. The dead layer of the Ge detector, however, had to be made considerably thicker than the drawing in order to improve the accuracy of the simulated detection efficiency. Materials outside of the detectors such as supporting frames and the sample itself were not taken into account in the simulation.

Simulation results and discussion

Comparison with experimental singles spectra

Before going to the detailed discussion of simulation results, we first compare the experimental γ -ray spectrum for the standard γ -ray source of ^{152}Eu with the calculation in Fig. 3 both are taken at the source-to-detector distance of 25 cm. The differences of peak efficiencies between the experiment and calculation are shown in Table 1. The

Fig. 1 Four possible detector configurations for the multiple γ -ray detector array taken up here for CPAA. **a** Design A composed of six Ge detectors and six BGO shields, **b** Design B composed of six Ge detectors, **c** Design C composed of seven Ge detectors, and **d** Design D composed of five Ge detectors

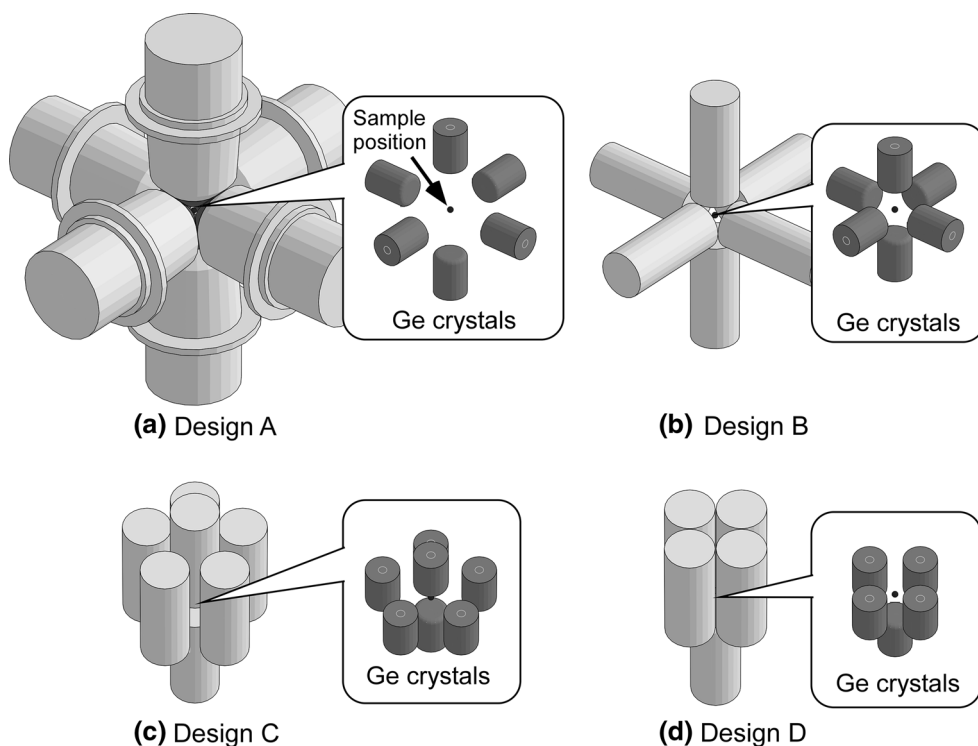


Fig. 2 Schematic sectional view for **a** Ge detector and **b** BGO anti-coincidence shield which were assumed in the simulation. The inner diameter, outer diameter and length of the BGO shield are 85, 160 and 220 mm, respectively

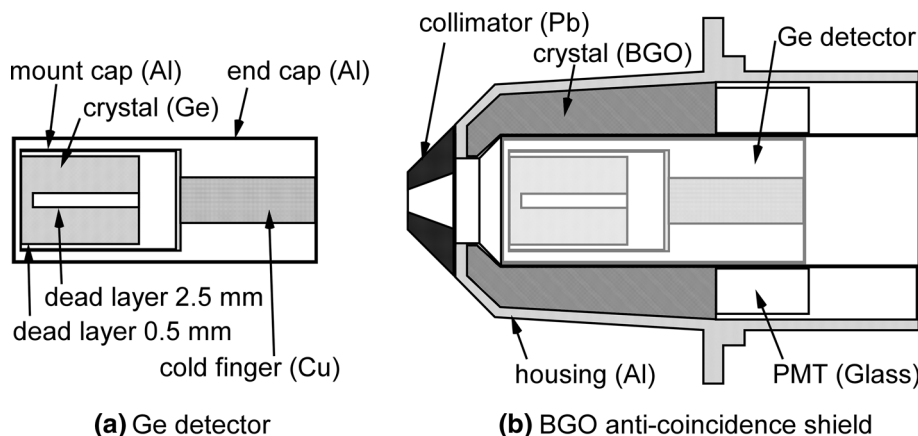


table shows that, while there is some deviation at low energy, the agreement is good taking account of the statistical error.

Total detection efficiency

The γ -ray detection efficiency at 1.33 MeV for a single detector at 5 cm from the source is calculated to be 0.56% from a γ -ray spectrum for ^{60}Co . The calculated detection efficiencies for the proposed design A, B, C, and D are 1.66, 3.79, 4.89, and 5.06%, respectively. In spite of the smallest number of detectors (5), the design D has the largest detection efficiency reflecting the close geometry. The averaged detection efficiencies of single detector for

each configuration are 0.29, 0.69, 0.81 and 1.17%, respectively.

These values are comparable with 1.5, 2.5, and 3.5% for GEMINI-II, STELLA (MPGA), and ANNRI, respectively in spite of the relatively small number of detectors included. The GEMINI-II array at the tandem accelerator facility in Tokai establishment in Japan atomic energy agency (JAEA) comprises sixteen BGO anti Compton spectrometers with 40–70% Ge detectors and three low energy photon spectrometers. The STELLA (MPGA) array in JRR-3 M guided neutron beam facility in JAEA is composed of eight BGO suppressed Clover detectors (120% relative efficiency) and four coaxial detectors (100% efficiency). Two BGO Compton suppressed

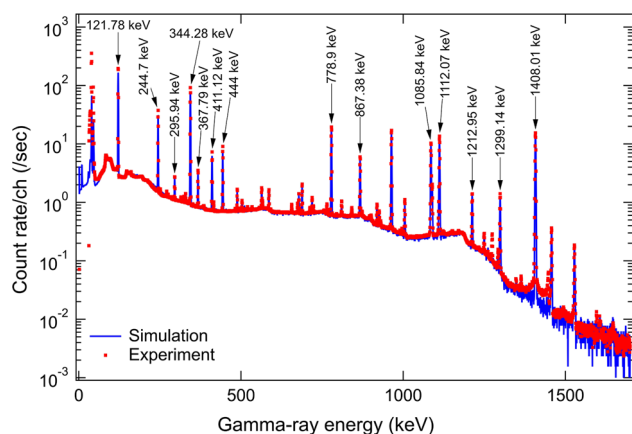


Fig. 3 Comparison of experimental and calculated singles γ -ray spectra for ^{152}Eu γ -ray source

Table 1 Difference between experiment and simulation for detection efficiency

γ -ray energy (keV)	Difference (%)
121.78	6.58 ± 0.17
244.7	0.6 ± 0.4
295.94	-0.4 ± 1.8
344.28	0.24 ± 0.24
367.79	0.9 ± 1.4
411.12	-1.5 ± 0.9
444	2.3 ± 0.8
778.9	1.5 ± 0.5
867.38	0.4 ± 0.9
964.1	1.1 ± 0.5
1085.84	0.2 ± 0.6
1112.07	1.8 ± 0.5
1212.95	-0.3 ± 1.7
1299.14	-0.3 ± 1.7
1408.01	1.4 ± 0.5

EURISYS Cluster detectors and eight BGO suppressed coaxial detectors are used in the ANNRI detector array at the beam line #4 in J-PARC in JAEA.

Signal-to-noise ratio

One dimensional spectra and two dimensional γ - γ matrices are created to evaluate the signal-to-noise ratio and the determination sensitivity from the γ - γ coincidence events generated by the Monte Carlo simulation calculation code Geant 4.10.2. Figure 4 shows a typical example of two dimensional γ - γ matrix obtained for the design A by assuming a ^{152}Eu standard source. The ^{152}Eu standard γ -ray source is chosen for two reasons. One is that it is

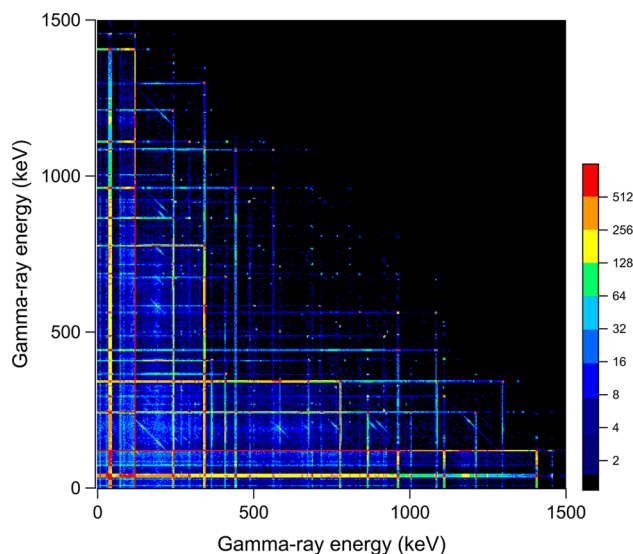


Fig. 4 A typical example of γ - γ two dimensional matrix obtained for the Design A by using a ^{152}Eu standard source

commercially available and can be used to obtain the experimental spectrum and matrix. The other is that it incorporates many γ -rays and coincident cascade γ -rays which are useful to evaluate the general features of signal-to-noise ratios. The decay scheme of ^{152}Eu is well established by many investigations and summarized in [42]. The level structure is irregular enough at the high-energy region to assure that favorable feature as a γ -ray source. The γ -ray intensity is known down to 10^{-3} order relative to the strongest 122.2 keV transition.

In the evaluation of signal-to-noise ratio, we take into account all the γ -ray cascades tabulated in the β^- decay data set of ^{152}Eu in NUDAT application developed in Brookhaven National Laboratory; the 52 gates and the 475 cascades have been included [42].

The signal-to-noise ratio is evaluated as the ratio $(A0-B0)/B0$ for the singles spectrum for a single detector at 10 cm from the sample. Here a peak gross count $A0$ for a specified transition with the energy E_γ is obtained by summing counts between $E_\gamma - 3$ and $E_\gamma + 3$ keV. A background count $B0$ is summed between $E_\gamma + 5$ and $E_\gamma + 11$ keV. The signal-to-noise ratios are derived for all the 36 transitions tabulated in [42].

The signal-to-noise ratio is given as the ratio $(A1-B1)/B1$ for the singles spectrum for a detector array. Here a peak gross count $A1$ for a specified transition and a background count $B1$ are defined in the same manner as above.

The signal-to-noise ratio for the two-dimensional spectrum is evaluated as $(A2-B2)/B2$. Here a peak gross count $A2$ for a specified cascade γ_1 - γ_2 is derived by summing counts in a rectangular region of $E_{\gamma_1} - 3$ to $E_{\gamma_1} + 3$ keV and $E_{\gamma_2} - 3$ to $E_{\gamma_2} + 3$ keV. A background count $B2$ is

summed in a rectangular region of $E\gamma_1 + 5$ to $E\gamma_1 + 11$ keV and $E\gamma_2 + 5$ to $E\gamma_2 + 11$ keV.

The improvement factor $IF(SN)$ of the signal-to-noise ratio for the two-dimensional spectrum relative to that of the singles spectrum is defined as

$$IF(SN) = \{(A2 - B2)/B2\} / \{(A0 - B0)/B0\} \quad (1)$$

and is shown in Fig. 5 for the 36 transitions from ^{152}Eu source tabulated in [42] as a function of γ -ray intensity. Data points scattering vertically originate from the $IF(SN)$ values obtained for a single transition gated by the different transitions in the cascade.

One important common feature in Fig. 5 is that the improvement factor is much dependent on the counterpart of the coincidence in the cascade of which the branching ratio and the γ -ray energy differ. Another feature is that we cannot find much dependence of $IF(SN)$ on the γ -ray intensities. The average values of the improvement factors are 177, 121, 112, and 155 for the design A, B, C, and D, respectively. Here the simulation has confirmed our earlier expectation that the design A may have the highest improvement for the signal-to-noise ratio.

Detection limit

When a nuclide with quantity, q , produces a peak in the singles spectrum of a single Ge detector (we may call it SS spectrum later), we can define the detection limit as

$$DL0 = 3q\sqrt{B0} / (A0 - B0) \quad (2)$$

Here we take 3 times the standard deviation for the detection limit.

Also the detection limit deduced from the summed singles spectrum of the γ -ray detector array (we may call it SA spectrum later) is defined as

$$DL1 = 3q\sqrt{B1} / (A1 - B1) \quad (3)$$

Similarly we can define the detection limit obtained from the two dimensional spectrum of the γ -ray detector array (we may call it MA spectrum later) as

$$DL2 = 3q\sqrt{B2} / (A2 - B2) \quad (4)$$

Then the improvement factor of $IF1(DL)$ and $IF2(DL)$ for the SA and MA spectra relative to the SS are defined as follows, respectively.

$$IF1(DL) = DL0 / DL1 \quad (5)$$

$$IF2(DL) = DL0 / DL2 \quad (6)$$

The improvement factor $IF1(DL)$ is shown in Fig. 6 for the 36 transitions from ^{152}Eu tabulated in [42] as a function of γ -ray intensity. The averaged values are 4.58, 5.15, 5.82, and 6.40 for the design A, B, C, and D, respectively. The improvement factor $IF2(DL)$ is shown in Fig. 7 for the same transitions as above. The averaged values are 1.31, 2.84, 3.69, and 3.93 for the design A, B, C, and D, respectively. Thus we conclude that the performance of the design D is the best on detection limit among them. Also we note the number (5) of Ge detectors of design D is the

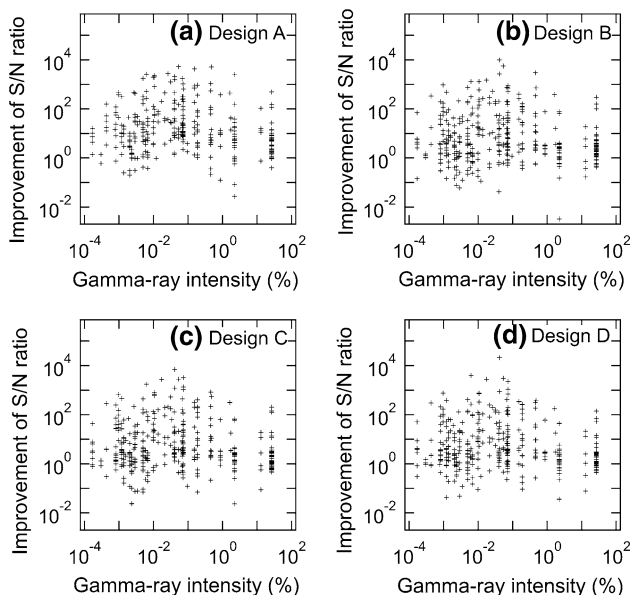


Fig. 5 Improvement of signal-to-noise ratio of **a** design A, **b** design B, **c** design C, and **d** design D, as a function of γ -ray intensity

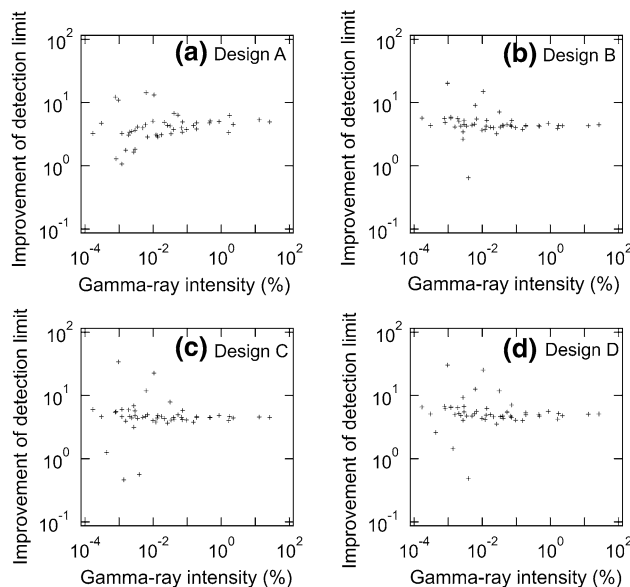


Fig. 6 Improvement of detection limit of **a** design A, **b** design B, **c** design C, and **d** design D, as a function of γ -ray intensity

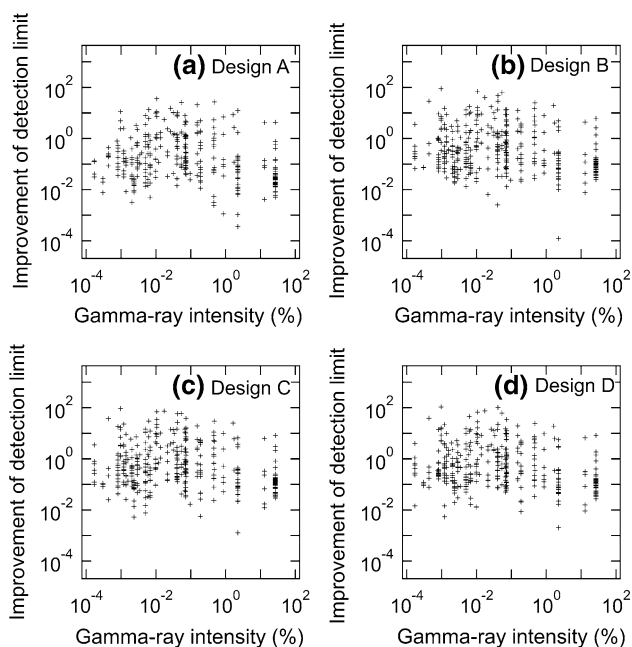


Fig. 7 Improvement of detection limit of **a** design A, **b** design B, **c** design C, and **d** design D, for two-dimensional spectrum as a function of γ -ray intensity

least of them that means the cost performance of the design D is the best as well.

Figure 8 show the typical γ -ray spectra; Blue line is the singles spectrum and red line is the projected spectrum gated by the 411 keV transition. The inset of the figure is the expanded portion of the spectra in the energy range between 600 and 1000 keV. The improvement of the signal-to-noise ratio and the detection limit is obvious in the figure. The peaks indicated by arrows in the inset are 678.6, 712.8, 794.8 and 937.1 keV transitions, showing the

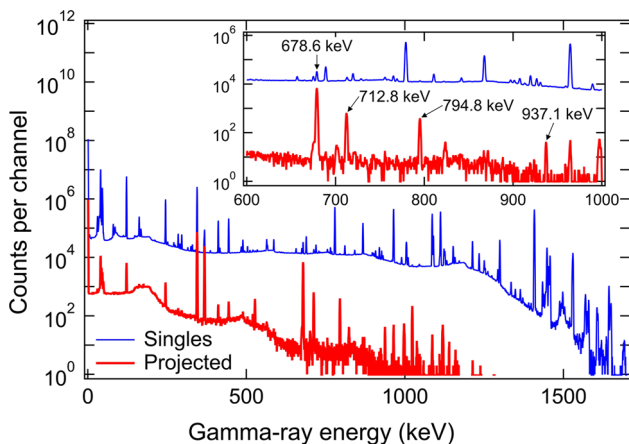


Fig. 8 Comparison of the singles spectrum and the projected spectrum gated by the 411 keV transition of ^{152}Eu . The inset shows the expanded portion of the spectra in the energy range between 600 and 1000 keV

improvement factors of the signal-to-noise ratio between 132 and 379 in the design D.

Based on the calculated improvement factors of the signal-to-noise ratio and detection limit we deduce general features of the merits attained by using the γ -ray detector array of design D: they are (1) the signal-to-noise ratio would be improved by a factor between 10^{-1} and 10^4 (155 on the average), (2) the detection limit would be improved by a factor between 10^{-3} and 10^2 (3.9 on the average), and (3) the improvement factors of the signal-to-noise ratio and detection limit of a single transition depend much on the counterpart of the coincidence in the cascade: by properly selecting the gate condition we attain the improvement factors better than one in most of the cases.

The following is a comment for the case of improvement factors less than one. If both the singles and γ - γ coincidence measurements are available, we are able to choose the one with better signal-to-noise ratio and detection limit. In that case the signal-to-noise ratio would be improved by a factor between 1 and 10^4 ; the detection limit would be improved by a factor between 6.4 and 10^2 .

Application to CPAA

As reviewed in [13], most elements (~ 65) can be analyzed among 85 stable elements including H-Bi, Th and U by CPAA. Since each element has plural stable nuclide[s], it amounts to 158 nuclides. However, the number of nuclides which emit cascade γ -rays is restricted to 116 nuclides.

As discussed in [13], most of the light elements with Z less than 20 are β^+ emitters which emit no γ -rays but 511 keV annihilation γ -rays. To analyze those elements, only a singles γ -ray measurement or multiple γ -ray measurement is not sufficient and we require radiochemical procedure coupled with CPAA. Although CPAA generally has the characteristics of non-destructive analysis, it is difficult for those elements.

The sensitivity of a singles γ -ray measurement for almost all the stable nuclides in CPAA is already described in [13]. Here we deduce the sensitivity of a multiple γ -ray measurement for three nuclides, and discuss their accuracy and detection limit.

We take up three nuclides of ^{111}Cd , ^{130}Te and ^{100}Ru , which transform to ^{111}In , ^{130}I and ^{100}Rh via the (p, n) reaction. Following the procedures of [13], we calculate for each nuclide the radioactivity after irradiating a single-element sample of 1 μg with an 8 MeV and 1 μA proton beam; where the irradiation time is set to the half life of each nuclide but not exceeding 10 h. The number of decays is then calculated by assuming the same cooling and measuring time as in [13]. We made for each nuclide the Geant 4 calculation based on the γ -ray detector array of

Table 2 Sensitivity of a multiple γ -ray measurement for three nuclides, accuracy and detection limit

Element	Produced nuclide (half life)	$E_{\gamma 1}$ (keV)	$E_{\gamma 2}$ (keV)	Number of decays	Peak counts	BG counts	Accuracy (%)	Detection limit (ng)
Cd	^{111}In (2.8 days)	245	171	2.6×10^6	8.0×10^4	8.2	1.1	0.11
Te	^{130}I (12 h)	669	536	1.0×10^7	4.5×10^4	21	1.4	0.03
Ru	^{100}Rh (21 h)	540	823	1.1×10^7	9.9×10^3	10	3.0	0.10

design D for the number of decays obtained above and derived a γ - γ matrix. From the γ - γ matrix we derive the peak and background counts for the most prominent peak of each nuclide. Table 2 is the summary of this analysis, showing the counts, accuracy and detection limit for the three nuclides.

The result shows that, in the present CPAA conditions, the peak counts are large enough for the element quantification. Due to the small background counts, the accuracy and detection limit are in the range of 1–3% and 0.03–0.11 ng, respectively. However we should note that in this calculation single-element samples of 1 μg were assumed and no matrix elements were included, which would cause background counts. Since element composition is much dependent on samples and accordingly background count is influenced by the composition, the accuracy and detection limit for actual samples need to be derived individually by taking into account the matrix elements. It will be made in forth coming papers.

Summary

For CPAA we take up four design candidates of a γ -ray detector array. By the radiation simulation code Geant 4.10.2, we investigated the performances of those detector candidates against the γ -rays emitted from ^{152}Eu γ -ray source. We first studied the response of a single detector. By adjusting the thickness of the dead layer of the Ge detector, we have succeeded in reproducing the experimental γ -ray singles spectrum.

Next, we derived one-dimensional spectra and two-dimensional matrices for the four candidates of a γ -ray detector array. By inspecting the signal-to-noise ratios and detection limits for those candidates, we have deduced the best design of the γ -ray detector array for CPAA, which is the one utilizing five bare germanium detectors in close geometry. This design also gives the best cost performance.

We have calculated the improvement factors of the signal-to-noise ratio and detection limit for all the known 52 transitions and 475 cascades in β^- decay of ^{152}Eu , and deduced general features of the merits attained by using the γ -ray detector array of the best design presented above: they are (1) the signal-to-noise ratio would be improved by

a factor of 155 on the average, (2) the detection limit would be improved by a factor of 3.9 on the average, and (3) the improvement factors of the signal-to-noise ratio and detection limit of a single transition depend much on the counterpart of the coincidence in the cascade: by properly selecting the gate condition we attain the improvement factors better than one in most of the cases.

Finally, in the application to CPAA analysis, we deduced the sensitivity of a multiple γ -ray measurement for three nuclides, their accuracy and detection limit. The result shows that the multiple γ -ray measurement is useful and applicable to 116 nuclides, which emit cascade γ -rays. The accuracy and detection limit, however, need to be studied individually for real samples, since background counts in the γ - γ matrix depend on the elemental composition.

Acknowledgements The authors appreciate the discussions by Drs. T. Hayakawa and Y. Hatsukawa of National Institutes for Quantum and Radiological Science and Technology. This work was supported in part by JSPS KAKENHI Grant Number 15K01357.

References

- Ricci E, Hahn RL (1965) Theory and experiment in rapid, sensitive ^3He activation analysis. *Anal Chem* 37:742–748
- Sanni AO, Roche NG, Dowell HJ, Schweikert EA, Ramsey TH (1984) On the determination of carbon and oxygen impurities in silicon by ^3He activation analysis. *J Radioanal Nucl Chem* 81:125–129
- Valladon M, Debrun JL (1977) Determination of oxygen in metals and semiconductors by means of the $^{16}\text{O}(\text{T}, \text{n})^{18}\text{F}$ reaction. *J Radioanal Nucl Chem* 39:385–395
- Debeve P, Do HP, Friedli C, Lerch P (1981) Trace determination of oxygen in gold copper alloys and in high purity gold using ^3He and ^4He activation analysis. *J Radioanal Nucl Chem* 64:213–223
- Bottger ML, Birnstein D, Helbig W, Niese S (1980) Removal of disturbances in carbon determination by activation analysis for lowering the detection limit. *J Radioanal Nucl Chem* 58:173–181
- Yagi M, Masumoto K (1985) Simultaneous determination of Ti, Cr, Fe, Cu, Ga and Zr in aluminium alloys by charged-particle activation analysis using the internal standard method. *J Radioanal Nucl Chem* 91:379–387
- Masumoto K, Yagi M (1985) Determination of strontium in biological materials by charged-particle activation analysis using the stable isotope dilution method. *J Radioanal Nucl Chem* 91:369–378

8. Yagi M, Masumoto K, Muto M (1986) An automatic gamma-ray spectrometer equipped with a micro-robot for sample changing. *J Radioanal Nucl Chem* 98:31–38
9. Yagi M, Masumoto K (1987) Instrumental charged-particle activation analysis of several selected elements in biological materials using the internal standard method. *J Radioanal Nucl Chem* 111:359–369
10. Shikano K, Yonezawa H, Shigematsu T (1993) Charged particle activation analysis of light elements at sub-ppb level. *J Radioanal Nucl Chem* 167:81–88
11. Chaturvedula CS, Banerjee A, Sauvage T, Courtois B, Duval F (2016) Application of 12 MeV proton activation to the analysis of archaeological specimens. *J Radioanal Nucl Chem* 308:241–249
12. Datta J, Dasgupta S, Guin R, Venkatesh M, Suvarna S, Chowdhury DP (2016) Determination of total arsenic and speciation of As(III) and As(V) in ground water by charged particle activation analysis. *J Radioanal Nucl Chem* 308:927–933
13. Oshima M, Yamaguchi Y, Muramatsu W, Amano H, Bi C, Seto H, Bamba S, Morimoto T (2016) Study of charged particle activation analysis (I): determination sensitivity for single element samples. *J Radioanal Nucl Chem* 308:711–719
14. PET <http://www.jcpet.jp/1-3-4-1/>. Accessed 19 Jun 2017
15. Lee IY (1990) The gammasphere. *Nucl Phys A520*:c641–c655
16. Wangen LE, Gladney ES, Starner JW, Hensley WK (1980) Determination of selenium in environmental standard reference materials by a gamma–gamma coincidence method using lithium-drifted germanium detectors. *Anal Chem* 52:765–767
17. Jakubek J, Nuiten P, Pluhar J, Pospisil S, Sinor M, Stekl I, Timoracky S, Vobecky M (1998) Coincidence gamma–gamma spectroscopy system for instrumental neutron activation analysis. *Nucl Instr Method A414*:261–264
18. Oshima M (2000) Non destructive trace element analysis. *Look Japan* 46:30–31
19. Hatsukawa Y, Oshima M, Hayakawa T, Toh Y, Shinohara N (2001) Application of multidimensional spectrum analysis for neutron activation analysis. *J Radioanal Nucl Chem* 248:121–124
20. Toh Y, Oshima M, Hatsukawa Y, Hayakawa T, Shinohara N (2001) Comparison method for neutron activation analysis with γ – γ matrix. *J Radioanal Nucl Chem* 250:373–376
21. Oshima M, Toh Y, Hatsukawa Y, Hayakawa T, Shinohara N (2002) A high-sensitivity and non-destructive trace element analysis based on multiple gamma-ray detection. *J Nucl Sci Technol* 39:292–294
22. Hatsukawa Y, Oshima M, Hayakawa T, Toh Y, Shinohara N (2002) Application of multiparameter coincidence spectrometry using a Ge detectors array to neutron activation analysis. *Nucl Instrum Methods A* 482:328–333
23. Oshima M, Toh Y, Hayakawa T, Hatsukawa Y, Shinohara N (2002) Development of a new method of neutron activation analysis with multiple gamma-ray detection—a high-sensitivity and non-destructive trace element analysis. *J Nucl Sci Tech Suppl* 2:1369–1371
24. Toh Y, Hatsukawa Y, Oshima M, Shinohara N, Hayakawa T, Kushita K, Ueno T (2002) Isotopic ratio of $^{129}\text{I}/^{127}\text{I}$ in seaweed measured by neutron activation analysis with γ – γ coincidence. *Health Phys* 83:110–113
25. Hatsukawa Y, Toh Y, Oshima M, Hayakawa T, Shinohara N, Kushita K, Ueno T, Toyota K (2003) New technique for the determination of trace elements using multiparameter coincidence spectrometry. *J Radioanal Nucl Chem* 255:111–113
26. Kimura A, Toh Y, Oshima M, Hatsukawa Y, Goto J (2007) Determination of As and Sb in iron and steel by neutron activation analysis with multiple gamma-ray detection. *J Radioanal Nucl Chem* 271:323–327
27. Hatsukawa Y, Miyamoto Y, Toh Y, Oshima M, Gharai MHM (2007) Determination of trace elements using multi-parameter coincidence spectrometry. *J Radioanal Nucl Chem* 271:43–45
28. Kimura A, Toh Y, Oshima M, Hatsukawa Y (2008) Lower limit of determination values for trace elements in iron certified reference materials by neutron activation analysis with multiple gamma-ray detection. *J Radioanal Nucl Chem* 278:521–525
29. Oshima M, Toh Y, Hatsukawa Y, Koizumi M, Kimura A, Haraga A, Ebihara M, Sushida K (2008) Multiple gamma-ray detection method and its application to nuclear chemistry. *J Radioanal Nucl Chem* 278:257–262
30. Jorgensen UG, Appel PWU, Hatsukawa Y, Frei R, Oshima M, Toh Y, Kimura A (2009) The earth–moon system during the late heavy bombardment period—geochemical support for impacts dominated by comets. *Icarus* 204:368–380
31. Oshima M, Toh Y, Kimura A, Ebihara M, Oura Y, Itoh Y, Sawahata H, Matsuo M (2007) Multiple prompt gamma-ray analysis and construction of its beam line. *J Radioanal Nucl Chem* 271:317–321
32. Toh Y, Koizumi M, Oshima M, Kimura A, Hatsukawa Y, Osa A, Goto J (2007) Analysis of toxic elements by MPGA. *J Radioanal and Nucl Chem* 272:303–305
33. Toh Y, Oshima M, Koizumi M, Kimura A, Hatsukawa Y (2008) Development of multiple prompt gamma-ray analysis. *J Radioanal Nucl Chem* 276:217–220
34. Toh Y, Oshima M, Koizumi M, Osa A, Kimura A, Goto J, Hatsukawa Y (2006) Analysis of cadmium in food by multiple prompt γ -ray spectroscopy. *Appl Radiat Isot* 64:751–754
35. Oura Y, Watanabe R, Ebihara M, Murakami Y, Toh Y, Kimura A, Koizumi M, Furutaka K, Oshima M, Hara K, Kin T, Nakamura S, Harada H (2012) Application of multiple prompt gamma-ray analysis (MPGA) to geochemical and cosmochemical samples. *J Radioanal Nucl Chem* 291:335–339
36. Shozugawa K, Matsuo M, Sano Y, Toh Y, Murakami Y, Furutaka K, Koizumi M, Kimura A, Hara K, Kin T, Oshima M, Nakamura S, Harada H (2012) Chemical composition of sediments from marine shallow-water hydrothermal mounds in Wakamiko submarine crater revealed by multiple prompt gamma-ray analysis. *J Radioanal Nucl Chem* 291:341–346
37. Furuno K, Oshima M, Komatsubara T, Furutaka K, Hayakawa T, Kidera M, Hatsukawa Y, Matsuda M, Mitarai S, Shizuma T, Saitoh T, Hashimoto N, Kusakari H, Sugawara M, Morikawa T (1999) A γ -ray detector array for joint spectroscopy experiments at JAERI tandem booster. *Nucl Instr Method A421*:211–226
38. Geant 4. <http://geant4.cern.ch/>. Accessed 19 June 2017
39. Agostinelli S et al (2003) Geant 4—a simulation toolkit. *Nucl Instr Method A506*:250–303
40. Allison J et al (2006) Geant 4 developments and applications. *IEEE Trans Nucl Sci* 53:270–278
41. Allison J et al (2016) Recent developments in Geant 4. *Nucl Instr Method A835*:186–225
42. NuDat. <http://www.nndc.bnl.gov/nudat/>. Accessed 19 Jun 2017